Uranium(VI) Adsorption and Surface Complexation Modeling onto Background Sediments from the F-Area Savannah River Site

Wenming Dong, Tetsu K. Tokunaga, James A. Davis, and Jiamin Wan*

Earth Sciences Division, Lawrence Berkeley National Laboratory, Berkeley, California

Supporting Information

ABSTRACT: The mobility of an acidic uranium waste plume in the F-Area of Savannah River Site is of great concern. In order to understand and predict uranium mobility, U(VI) adsorption experiments were performed as a function of pH using background F-Area aquifer sediments and reference goethite and kaolinite (major reactive phases of F-Area sediments), and a component-additivity (CA) based surface complexation model (SCM) was developed. Our experimental results indicate that the fine fractions (≤45 μm) in sediments control U(VI) adsorption due to their large surface area, although the quartz sands show a stronger adsorption ability per unit surface area than the fine fractions at pH < 5.0. Kaolinite is a more important sorbent for U(VI) at pH < 4.0, while goethite plays a major role at pH > 4.0. Our CA model combines an existing U(VI) SCM for goethite and a modified U(VI) SCM for kaolinite along with estimated relative surface area abundances of these component minerals. The modeling approach successfully predicts U(VI) adsorption behavior by the background F-Area sediments. The model suggests that exchange sites on kaolinite dominate U(VI) adsorption at pH < 4.0, goethite and kaolinite edge sites cocontribute to U(VI) adsorption at pH 4.0−6.0, and goethite dominates U(VI) adsorption at pH > 6.0.

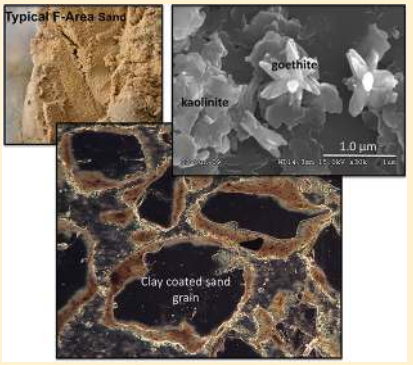

INTRODUCTION

The Savannah River Site (SRS) was one of the major U.S. Department of Energy (DOE) facilities for plutonium production during the Cold War. Acidic waste solutions containing low-level radioactivity from numerous isotopes were discharged to a series of unlined seepage basins in the F-Area of the SRS during 1955−1989. Although the site has gone through many years of active remediation, the groundwater remains acidic, and the concentrations of U(VI) and other radionuclides are still significantly higher than their Maximum Contaminant Levels (MCLs).[1−3] The mobility of U(VI) is of great concern in the SRS F-Area groundwater, and the prediction of U(VI) mobility requires a reactive transport model capable of simulating U(VI) adsorption by aquifer sediments using a surface complexation model (SCM) that has been demonstrated to be successful over the range of site-specific geochemical conditions.[4]

U(VI) adsorption onto mineral surfaces plays a key role in controlling its mobility in groundwater.[1] Our studies [1,3] have shown that the SRS F-Area sediments are composed predominantly of quartz sand with varying amounts of fine-grained minerals (≤45 μm, 2−13%). Goethite and kaolinite were identified as the major mineral components of the fine fractions, residing primarily as associated material on sand grains (Figure 1c). The variation of groundwater pH (3.0−5.5) in the F-Area is another key factor, which can greatly affect U(VI) adsorption behavior because U(VI) adsorption extent is strongly pH-dependent, especially under acidic pH conditions.[1,5−8] Therefore, investigations of pH-dependent U(VI) adsorption behavior onto the sediment size fractions and goethite and kaolinite are necessary for understanding and modeling U(VI) adsorption behavior onto SRS F-Area sediments.

The objectives of this study were to investigate the adsorption behavior of U(VI) onto background F-Area sediments and their size fractions as a function of pH and to compare the results with U(VI) adsorption onto reference goethite and kaolinite minerals. Using a component additivity (CA) modeling approach,[4] the U(VI) adsorption data were used to develop a SCM that is capable of predicting U(VI) adsorption behavior onto F-Area sediments, based on the variable content of goethite and kaolinite.

MATERIALS AND METHODS

Sediments, Goethite and Kaolinite. Two background sediment samples (A and B) were collected from a borehole at a depth of 21.7 and 23.7 m below the surface, respectively, near the contaminated F-Area of the U.S. DOE's SRS.[3] The two sediments are from within the same stratum and are composed of the same major minerals as contaminated F-area sediments.[3] The samples were moisture-preserved in double sealed polypropylene plastic bags and stored in a 4 °C refrigerator until use.

The selected properties of sediments-A and -B are presented in Table 1. The samples were composed predominantly of fine quartz sand, with about 13.0% and 5.5% fine fraction (≤45 μm) in sediment-A and -B, respectively. The fine and coarse fractions of the samples were separated via wet sieving using deionized water (Figure 1b). Measured U concentrations and pH values

Received: October 12, 2011
Revised: December 15, 2011
Accepted: December 19, 2011
Published: December 19, 2011

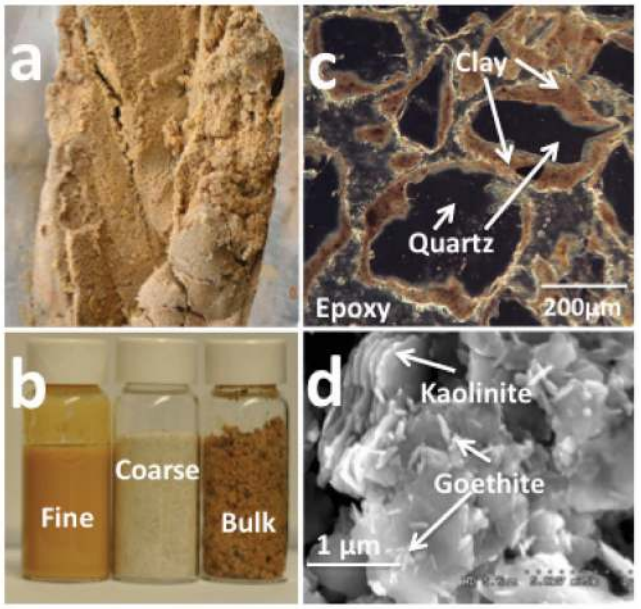

Figure 1. (a) Typical sediments from upper aquifer in SRS F-Area; (b) the bulk sediment-A can be readily separated into the fine fraction (≤45 μm) and coarse fraction (>45 μm); (c) optical microscope image of bulk sediment-A; and (d) scanning electron micrograph of the fine fraction of sediment-A.

Table 1. Selected Properties of Sediment Samples from SRS F-Area

Bulk Sediment	Sample-A	Sample-B
Specific surface area (SSA) (m^2/g)	4.62 ± 0.30	1.90 ± 0.10
[a] pH	5.4	5.3
[b] U in solid sediment (μg/g)	0.006	0.014
Fine Fraction (≤45 μm)	~13.0%	~5.5%
Coarse Fraction (>45 μm)	~87.0%	~94.5%
Fine Fraction:		
SSA (m^2/g)	35.9 ± 1.8	33.6 ± 1.7
[c] Goethite (wt%)	~17%	~27%
[d] Kaolinite (wt%)	~83%	~73%
[e] TIC (mg/g)	<0.001	<0.001
[f] TOC (mg/g)	0.64	0.55
Coarse Fraction:		
SSA (m^2/g)	0.08 ± 0.01	0.18 ± 0.02
Reference Mineral:	Goethite	Kaolinite
SSA (m^2/g)	16.2 ± 1.0	20.6 ± 1.2

[a]Measured with 1:1 ratio of fresh sediment to deionized water. [b]Extractable U by pH = 9.5 carbonate buffer solution;[39] [c]Estimated by assuming that all measured Fe using XRF (X-ray fluorescence) was from goethite (FeO(OH)). [d]Estimated by assuming that all measured Al using XRF was from kaolinite ($Al_2Si_2O_5(OH)_4$); [e]Total inorganic carbon; [f]Total organic carbon.

in the samples are at background levels, indicating that the collected samples were not contaminated by the acidic, U-containing plume. Kaolinite and goethite were identified as the major minerals of the fine fractions by X-ray diffraction (XRD),[3] and were closely associated with the quartz grains upon drying (Figure 1). For comparison, reference goethite and kaolinite from Alfa Aesar (Ward Hill, MA) were used as model minerals, with N_2–BET specific surface areas (SSA) of 16.2 and 20.7 m^2/g, respectively.

Stock Suspensions and Solutions. Prior to their use in batch experiments, the fine-fractions of sediments-A and -B, reference goethite or kaolinite were suspended in deionized water as stock suspensions (25 g/L). U(VI) stock solution (25 μM) was prepared by dilution of a U plasma emission standard (10 g/L) with deionized water, and the pH was adjusted to 3.0 with 0.1 N HNO_3 to prevent U(VI) precipitation. Other stock solutions were prepared using ACS reagent grade or higher.

U(VI) Adsorption Experiments. Batch U(VI) adsorption experiments were conducted in duplicate as a function of pH (3.0 − 8.5) under conditions of a constant total U(VI) concentration (1.0 μM) in 0.01 M $NaNO_3$ solution under atmospheric CO_2(g) ($P_{CO2} = 10^{-3.5}$ atm) and at ambient temperature (22.5 °C). The solution ionic strength was selected to be similar to that of the background groundwater in the F-Area. Fifteen mL polypropylene centrifuge tubes containing 10 mL solution were used for goethite, kaolinite, and fine fractions with a solid concentration of 5 g/L. Fifty mL polypropylene centrifuge tubes containing 40 mL solution were used for bulk sediments (20 g/L solid) and coarse fractions (100 g/L). For solution pH > 5.5, a precalculated amount of $NaHCO_3/Na_2CO_3$ stock solution was added to equilibrate with atmospheric CO_2(g). For pH ≤ 5.5, HNO_3 (0.1 M) and NaOH/$NaHCO_3$ (0.1M) were used to adjust pH to the desired values. All samples were maintained in equilibrium with atmospheric CO_2(g) by frequent exposure to air. The pH values were monitored and adjusted daily with small amounts of NaOH/$NaHCO_3$ or HNO_3 solutions until the pH shifts were <0.05 pH unit. The suspensions were placed on a shaker for 3 days to reach equilibrium,[1] after which the final pH values of the suspensions were measured using an Orion 8104BNUWP Ross Ultra pH electrode. An aliquot (2 mL) of each suspension was filtered using 0.2 μm polysulfone membrane syringe filters (National Scientific Company, Duluth, GA), and the first 0.5 mL of filtrate was discarded. The filtrate was acidified with 1% HNO_3 and analyzed for U and other elements by inductively coupled plasma mass spectrometry (ICP-MS).

Modeling. The geochemical computer code PHREEQC[9] was used for calculation and modeling of U(VI) speciation and adsorption. Electrostatic SCMs (containing electrical double layer correction terms in the mass law for adsorption reactions) for goethite and kaolinite were selected/modified from existing literature to describe our experimental data for U(VI) adsorption onto the reference minerals, goethite and kaolinite (Table 2). A component-additivity approach[4] was then used, with goethite and kaolinite as adsorbing component minerals, to predict U(VI) adsorption behavior by the F-Area sediment samples. The relevant aqueous reactions and constants used are given in Table S1 of the Supporting Information (SI)).

In our modeling, we assumed that all sorbents have the same thickness of electrostatic diffuse layer (10 nm) and the surface charges were counterbalanced in the diffuse layer with the counterions only.[9] For the mixed mineral assemblages (e.g., the fine fractions of sediments-1A and 1B), the PHREEQC code can simulate U(VI) adsorption to different mineral components while also providing their specific surface charges.

■ RESULTS AND DISCUSSION

In this work, different solid concentrations with different specific surface areas were used for U(VI) adsorption studies. To directly compare their adsorption extent and evaluate adsorption additivity,[10−12] the experimental data are reported both as mass and surface area based distribution coefficients, K_d (mL/g) or K_a (mL/m^2) (Figure 2). To illustrate the relative contributions of

individual mineral and specific surface species for the overall adsorption of U(VI), the surface complexation modeling data along with the experimental data are presented in adsorption percentages (Figures 3 and 4).

U(VI) Adsorption Data. *Comparison of U(VI) Adsorption onto Fine, Coarse, and Bulk Sediments.* Figure 2a shows that U(VI) adsorbed more strongly to the fine fraction than to the coarse fraction on a unit mass basis. U(VI) adsorption to the bulk sediment-A was intermediate between the fine and coarse fractions and was in good agreement with the amount calculated by a mass fraction based linear additivity approach (solid line in Figure 2a), i.e., $K_{d(bulk)} = K_{d(fine)}\, f_{(fine)} + K_{d(coarse)} f_{(coarse)}$,

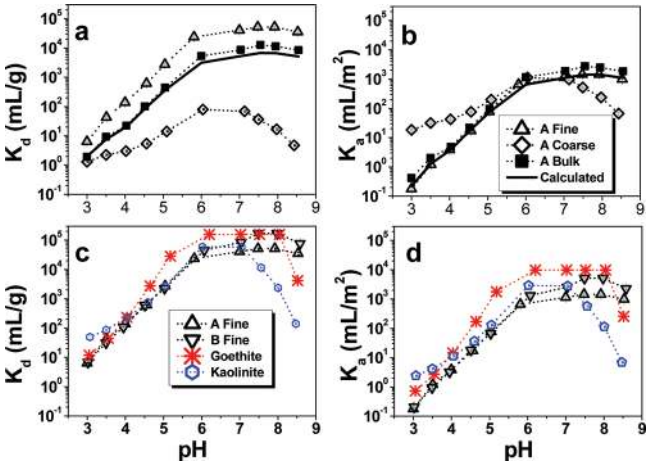

Figure 2. The mass-normalized (a and c) versus surface-area-normalized (b and d) distribution coefficients of U(VI). (a) and (b): Comparison of U(VI) adsorption onto the fine, coarse and bulk samples of sediment-A. (c) and (d): Comparison of U(VI) adsorption onto the fine fractions of sediments-A and -B, reference goethite and kaolinite. Symbols are experimental data points with estimated uncertainties. The dashed lines show the data trends, and the bold solid lines are calculated data.

where $f_{(fine)}$ and $f_{(coarse)}$ are the mass fractions of the fine and coarse fractions in the bulk sediment-A (Table 1), respectively. $K_{d(fine)}$, $K_{d(coarse)}$, and $K_{d(bulk)}$ are the mass-based K_d (mL/g) in the fine, coarse and bulk sediment systems. When the same adsorption data in Figure 2a are replotted per unit surface area (Figure 2b), the coarse fraction was found to have much stronger adsorption capacity (larger K_a, mL/m^2) than the fine fraction at pH < 5.0. This behavior can be explained by the amphoteric nature of mineral surfaces. The coarse fraction is composed of quartz sand (Figure 1) with a point of zero charge (PZC) at pH ≈ 2.0−3.0,[13] and the quartz surfaces are net negatively charged at pH 3.0−5.0, adsorption of the positively charged aqueous UO_2^{2+} species (Figure S1 of the SI) is enhanced by electrostatic attraction. In contrast, the fine fraction surfaces are mainly composed of kaolinite and goethite minerals with a PZC at pH ≈ 5.0 for kaolinite,[14] and a PZC at pH ≈ 9.2 for goethite.[15] Thus, these minerals are net positively charged at pH 3.0−5.0, which can depress UO_2^{2+} adsorption. Due to these electrostatic differences, there is a greater dependence of the fine fraction on the electrical double layer as a function of pH (at low pH), which is apparent in the K_a versus pH plot (Figure 2b). Nonetheless, the surface area fraction based linear additivity approach (solid line in Figure 2b) suggests that ~100% of U(VI) uptake by bulk sediment-A was contributed by the fine fraction (SSA 35.9 m^2/g in sediment-A); the relative contribution from the coarse fraction was small or negligible under our experimental conditions because of its very low SSA (0.08 m^2/g). The calculation was made by $K_{a(bulk)} = K_{a(fine)}\{f_{(fine)}\, SSA_{(fine)}/(f_{(fine)}\, SSA_{(fine)} + f_{(coarse)}\, SSA_{(coarse)})\} + K_{a(coarse)}\{f_{(coarse)}\, SSA_{(coarse)}/(f_{(fine)}\, SSA_{(fine)} + f_{(coarse)}\, SSA_{(coarse)})\}$, where $K_{a(bulk)}$, $K_{a(fine)}$, and $K_{a(coarse)}$ are the surface area based distribution coefficients (mL/m^2) of U(VI) for the bulk, fine and coarse sediments (Figure 2b), respectively; $SSA_{(fine)}$ and $SSA_{(coarse)}$ are the specific surface area (m^2/g) of the fine and coarse fractions (Table 1), respectively. Similar results were observed for bulk sediment-B and its fine and coarse fractions, suggesting that the grain size fraction additivity approach can be applied to make an approximate prediction of the overall U(VI) adsorption binding onto the F-Area bulk sediment samples.

Comparison of U(VI) Adsorption onto Goethite, Kaolinite and the Fine Fractions of Sediments. The distribution coefficients of U(VI) adsorption with the fine fractions of sediments-A and -B and reference goethite and kaolinite are shown in Figure 2c (unit mass) and Figure 2d (unit surface area). Both Figure 2c,d indicate that U(VI) adsorption to kaolinite is stronger than to goethite at pH < 4.0, while U(VI) adsorption to goethite is stronger than to kaolinite at pH > 4.0. The stronger adsorption by kaolinite at pH < 4.0 can be attributed partly to the contribution of ion exchange sites of the kaolinite, which can adsorb heavy metal ions strongly (e.g., UO_2^{2+}, Cu^{2+}, and Pb^{2+}) at low ionic strength (0.01 M $NaNO_3$) and low pH conditions.[5,7,14,16,17] The strong adsorption by goethite at pH > 4.0 is consistent with many observations in the literature, where iron (oxy)hydroxides such as amorphous iron hydroxide, ferrihydrite and goethite in aquifer sediments have been identified as major sinks for U(VI).[6,13,15,18−20]

Compared to the fine fractions (Figure 2c,d), kaolinite exhibits stronger U(VI) adsorption at pH < 4.0 and a similar adsorption extent at pH > 4.0 (up to 7.0), and goethite shows a similar adsorption extent at pH < 4.0 and stronger adsorption at pH > 4.0 (up to 8.0). These observations are contrary to expectations, i.e., adsorption data for the fine fractions should be intermediate between the reference goethite and kaolinite, since the fine fractions are mainly composed of these minerals. The disagreement is likely due to the influence of solution chemistry on U(VI) adsorption. Concentrations of cations such as Al^{3+}, Ca^{2+}, Mg^{2+}, Na^+, and K^+, as well as Si measured by ICP-MS were significantly greater in the solutions of the fine fraction experiments than those in reference goethite and kaolinite systems (Table S2 in SI). The higher concentrations of these elements in the fine fraction experiments are due to ion exchange or other sediment-water reactions that release the elements to solution. These coexisting ions can decrease U(VI) adsorption by formation of aqueous U(VI) complexes [10,21−24] or by competitive adsorption reactions.[5,7] Because of the variations in U(VI) aqueous chemistry in the experiments, development of a SCM-CA model capable of describing U(VI) adsorption behavior under various geochemical conditions will be highly valuable in describing U(VI) reactive transport in the SRS F-Area.

Surface Complexation Modeling. *U(VI)/Goethite.* As an initial attempt to simulate the U(VI) experimental data with goethite, we first selected and tested the widely cited SCM proposed by Waite et al.,[6] and the recently updated SCM by Mahoney et al.[25] However, application of these two SCMs tended to overpredict the amount of U(VI) adsorption under

Table 2. Selected Surface Reactions and Constants for Reference Goethite and Kaolinite[a]

Goethite	log K
(1). 2 >FeOH$^{-0.5}$ + UO_2^{2+} = $(>FeOH)_2UO_2^{+}$	14.11[b]
(2). 2 >FeOH$^{-0.5}$ + UO_2^{2+} + H_2CO_3 = $(>FeOH)_2UO_2CO_3^{-}$ + 2 H^+	4.35[b]
(3). >FeOH$^{-0.5}$ + H^+ = >FeOH$^{+0.5}$	9.18[b]
(4). 2 >FeOH$^{-0.5}$ + H_2CO_3 = $(>FeO)_2CO_2^{-1}$ + 2H_2O	5.93[b]
(5). >FeOH$^{-0.5}$ + H_2CO_3 + Na^+ = >FeO$CO_2^{-1.5}Na^+$ + H^+ + H_2O	−3.02[b]
Kaolinite	
(6). 2 >SOH$^{-0.5}$ + UO_2^{2+} = $(>SOH)_2UO_2^{+}$	5.3[c]
(7). 2 >SOH$^{-0.5}$ + UO_2^{2+} + H_2CO_3 = $(>SOH)_2UO_2CO_3^{-}$ + 2 H^+	−0.1[c]
(8). >SOH$^{-0.5}$ + H^+ = >$SOH_2^{+0.5}$	4.9[d]
(9). >SOH$^{-0.5}$ + Na^+ = >SOH-$Na^{+0.5}$	−2.1[d]
(10). >SOH$^{-0.5}$ + H^+ + NO_3^- = >SOH_2–$NO_3^{-0.5}$	4.9[d]
(11). 2 >X$^-$ + UO_2^{2+} = $(>X)_2UO_2$	7.1[e]
(12). >X$^-$ + Na^+ = >XNa	2.9[d]
(13). >X$^-$ + H^+ = >XH	4.5[e]
(14). 2 >X$^-$ + Ca^{2+} = $(>X)_2Ca$	6.8[e]
(15). 3 >X$^-$ + Al^{3+} = $(>X)_3Al$	8.0[e]

[a]Goethite edge site (>FeOH) density =3.0/nm^2 from Sherman et al.;[15] kaolinite exchange site (>X$^-$) density = 0.28/nm^2 and the edge site (>SOH) density = 2.3/nm^2 from Heidmann et al.[14,35] [b]Sherman et al.[15] [c]This work. [d]Heidmann et al.[14,35] [e]Obtained by modifying the log K values from the same and similarly charged cation exchange reactions in Heidmann et al.[14,35]

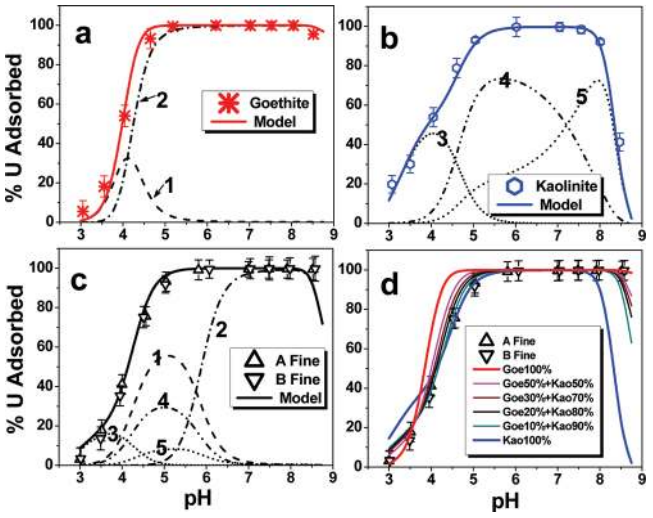

Figure 3. Surface complexation modeling of U(VI) adsorption onto (a) goethite, (b) kaolinite, (c) the fine fractions of sediments-A and -B by using 17% of overall surface area is contributed by goethite and the remaining surface area (83%) is from kaolinite, and (d) the sensitivity analysis of modeling fits as a function of the relative surface contribution from goethite and kaolinite for U(VI) adsorption to the fine fractions of sediments-A and -B. Symbols are experimental data points with estimated uncertainties. The solid lines are the overall model fits and the dashed lines are the fitted distribution of specific surface species: 1 = $(>FeOH)_2UO_2^{+}$, 2 = $(>FeOH)_2UO_2CO_3^{-}$, 3 = $>X_2UO_2$, 4 = $(>SOH)_2UO_2^{+}$, and 5 = $(>SOH)_2UO_2CO_3^{-}$. Note: the measured coexisting ions in Table S2 in SI were included in modeling for their relevant ion exchange reactions (Table 2) and aqueous complexation reactions (Table S1 in SI).

low pH conditions (pH < 5.0). The failure of these SCMs to agree with our experimental data is likely due to different sorbent properties and experimental conditions, i.e., HFO was used by these authors whereas we used goethite in this study.

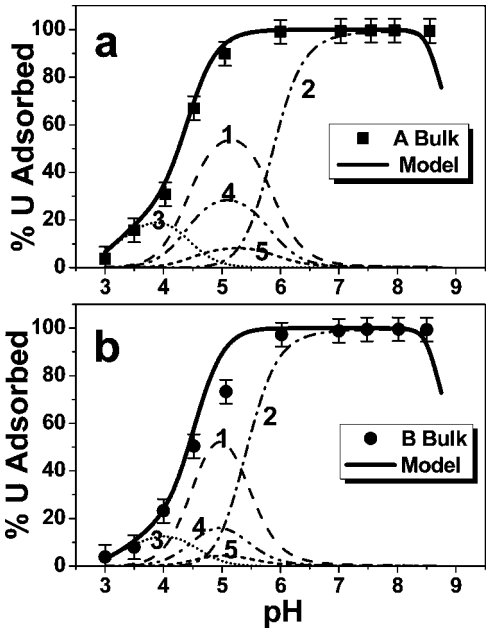

Figure 4. Surface complexation modeling of U(VI) adsorption onto bulk sediment-A (a) and sediment-B (b) as a function of pH. The solid line is the overall model fit and the dashed lines are the fitted distribution of specific surface species: 1 = $(>FeOH)_2UO_2^{+}$, 2 = $(>FeOH)_2UO_2CO_3^{-}$, 3 = $>X_2UO_2$, 4 = $(>SOH)_2UO_2^{+}$, and 5 = $(>SOH)_2UO_2CO_3^{-}$. Note: the measured coexisting ions in Table S2 in SI were included in modeling for their relevant ion exchange reactions (Table 2) and aqueous complexation reactions (Table S1 in SI).

Sherman et al.[15] developed an SCM specifically for U(VI) adsorption onto reference goethite using a 1-pK model for surface protonation[26] and a double layer or extended Stern model for surface electrostatics. In the model, one-site, >FeOH$^{-0.5}$, and three surface complexes, $(>FeOH)_2UO_2^{+}$, $(>FeOH)_2UO_2CO_3^{-}$, and $(>FeO)CO_2UO_2^{+0.5}$, were proposed based on their extended X-ray adsorption fine structure (EXAFS) spectra data; details are summarized in Table 2. Direct application of Sherman's SCM by input of surface reactions and parameters selected in Table 2 to the PHREEQC code, combined with the measured SSA of goethite (16.2 m^2/g), and inclusion of all U(VI) and other relevant aqueous reaction constants (Table S1 in SI), provides an excellent fit to our experimental data (Figure 3a). Although previous studies [27,28] have reported that the surface complexation constants are also dependent on the SSAs of sorbents, this study shows that direct use of the surface complexation constants from the Sherman et al. without any adjustment for differences in the SSAs of the goethite materials used are still effective. The goethite used by Sherman et al. with a SSA of 45 m^2/g and the goethite used in this study with a SSA of 16.2 m^2/g. Figure 3a indicates that the bidentate ternary uranyl-carbonate surface complex, $(>FeOH)_2UO_2CO_3^{-}$, dominates under our experimental conditions at pH > 4.0 and surface species, $(>FeOH)_2UO_2^{+}$, dominates at pH < 4.0. The surface complex, $(>FeO)CO_2UO_2^{+0.5}$, was not included in Table 2 and Figure 3a because its abundance is calculated to be negligible (<0.1%) under our experimental conditions using its surface complexation constant of log K = 6.24 from Sherman et al.[15] It is likely due to the difference of U(VI) loadings. U(VI) loading (0.005 wt %) in our experiment is much lower than those used by Sherman et al.'s lowest U(VI) loading (0.026 wt %).

U(VI)/Kaolinite. The SCM of U(VI) adsorption onto clay minerals was expected to be more complicated due to the presence of multiple surface sites.[5,7,29−31] Monodentate surface complexes have usually been proposed via reactions of clay edge surface sites with major U(VI) species in the aqueous phase.[5,7,30] For example, McKinley et al.,[5] Pabalan and Turner,[30] and Turner et al.[7] proposed the formation of monodentate surface complexes of aqueous UO_2^{2+} and $(UO_2)_3(OH)_5^+$ species with amphoteric edge sites and ion exchange sites of the montmorillonite surface. They assumed that the major aqueous U(VI) species (UO_2^{2+} and $(UO_2)_3(OH)_5^+$) were involved in the surface reactions. However, these studies did not provide any direct molecular structural evidence supporting the formation of the proposed surface complexes. Recently, several spectroscopic investigations have suggested that U(VI) species were adsorbed onto clay surfaces via bidentate surface complexes.[29,32] These authors investigated the molecular structure of U(VI) surface complexes on alumina, silica and montmorillonite using X-ray adsorption fine structure (XAFS), laser-induced fluorescence spectroscopy (LIFS), and X-ray photoelectron spectroscopy (XPS). These results suggested that adsorption of U(VI) species (e.g., aqueous UO_2^{2+} and $(UO_2)_3(OH)_5^+$) onto clay surfaces occurs via cation exchange at low pH and low ionic strength, and via formation of bidentate inner-sphere surface complexes at near-neutral pH conditions. However, these previous studies did not consider the potential formation of uranyl-carbonate ternary surface complexes on clay surfaces because their experiments were performed either under CO_2(g) free or low CO_2(g) conditions.[5,29,30,32] Recently, more detailed studies by Catalano and Brown Jr.[33] and Arai et al.[34] using EXAFS spectroscopy revealed that U(VI) adsorption onto montmorillonite and imogolite surfaces occurs as uranyl-carbonate ternary surface complexes in systems equilibrated with atmospheric CO_2. Formation of polymeric surface complexes via adsorption of aqueous $UO_2)_3(OH)_5^+$ was not observed, which is consistent with our calculation that at low U(VI) concentration ($\leq$1 μM) and in the presence of atmospheric CO_2, the formation of aqueous $UO_2)_3(OH)_5^+$ is not favored (Figure S1 in SI).

On the basis of the above spectroscopic observations and the similar adsorption sites of kaolinite and montmorillonite minerals, we modified the surface reactions and parameters for U(VI) adsorption onto kaolinite (Table 2). Our modeling approach is summarized by the following points: (i) U(VI) is adsorbed via formation of bidentate surface complexes; (ii) in addition to the UO_2^{2+} surface species ternary uranyl-carbonato surface complexes are formed. In agreement with our goethite system, we assumed that similar surface complexes (Table 2, i.e., $(>SOH)_2UO_2^+$, $(>SOH)_2UO_2CO_3^-$) are formed on the kaolinite amphoteric edge sites; (iii) for kaolinite, cation exchange sites ($>X^-$) and amphoteric edge sites (>SOH) with a 1-p*K* model were chosen based on the data of Heidmann et al.[14,35] The >SOH sites simply represent both silanol (>SiOH) and aluminol (>AlOH) sites on kaolinite surfaces. The treatment of amphoteric edge sites as a single surface site is generally recognized as a convenient modeling framework rather than a precise representation of actual functional groups existing at clay edge sites.[14,16,17,35] The overall surface site density was estimated to be ~2.3/nm^2 for >SOH and 0.28/nm^2 for $>X^-$ according to the reported values by Heidmann et al.,[14,35] which are in good agreement with other values in the literature;[36,37] (iv) ion exchange reactions must be included in U(VI) adsorption modeling at low ionic strength system, e.g., the 0.01 M $NaNO_3$ initial solution. Constrained by these considerations, modeling of U(VI) adsorption to kaolinite (Figure 3b) was completed using the reactions and parameters in Table 2 and Table S1 (SI) and the concentrations of coexisting ions in Table S2 in SI. The log *K* values for cation exchange reactions of 11-15 in Table 2 were first estimated from the log *K* ranges reported by Heidmann et al.[14,35] with the same and similar charged cations and then chosen based on the overall tests to fit our adsorption data at pH 3.0−4.0. Similarly, the log *K* values for reactions 6 and 7 in Table 2 were obtained based on the overall fitting results to our U(VI) adsorption data in the pH range of 4.0−6.0 for the complex $(<SOH)_2UO_2^+$, and in the pH range of 6.0−8.5 for the ternary complex of $(>SOH)_2UO_2CO_3^-$, respectively (Figure 3b). Figure 3b shows that the cation exchange sites in kaolinite contributed significantly to U(VI) adsorption at low pH.

U(VI)/Fine Fractions. The fine fractions of sediments-A and -B are mainly composed of goethite and kaolinite minerals, suggesting that a CA approach based on the SCMs of U(VI) derived from goethite and kaolinite (Table 2) may be applied to predict U(VI) adsorption data onto the fine fractions. The challenge is to estimate the relative surface area abundances of goethite and kaolinite in the total SSA of fine fractions.[4] Two estimates have been performed in this work. In the first approach, we assume that the relative surface area abundances of goethite and kaolinite in the fine fractions are the same as their weight abundances.[4,38] The weight abundances were estimated to be ~17% goethite and ~83% kaolinite for the fine fraction of sediment-A, and ~27% goethite and ~73% kaolinite for the fine fraction of sediment-B (Table 1). In the second approach, relative surface area abundances of goethite and kaolinite in the fine fraction of sediment-A were estimated using a humic acid adsorption method (see details in SI and ref 1). The interesting result of the latter method was that the overall surface contribution was estimated to be ~17% from goethite and ~83% from kaolinite, the same values as the estimated weight abundances. This suggests that the grain size distributions of goethite and kaolinite in the fine fraction of sediment-A are nearly the same, thus resulting in similar specific surface area values for those grains. Because of the agreement of the two methods, we assumed that ~17% of total SSA in the fine fractions was contributed by goethite and ~83% by kaolinite. With the combination of the SCMs and parameters in Table 2 and Table S1 in SI, the overall model calculation and the relative distribution of each specific surface species are presented in Figure 3c. Figure 3c indicates that the SCM-CA model can predict U(VI) adsorption behavior onto the fine fractions very well. It should be noted that the measured coexisting ions in Table S2 in SI were included for modeling in Figure 3c. Also not that the close model predictions of measurements were achieved despite the fact that the goethite (16.2 m^2/g) and kaolinite (20.7 m^2/g) specimens had lower SSA values than the sediment fine fractions (~35 m^2/g). This likely results from the fact that the goethite and kaolinite mineral specimens have fairly similar proportionally lower SSAs (~46% and ~60%, respectively) relative to that of the sediment fine fractions.

Sensitivity Analysis. In order to analyze the sensitivity of the modeling data with variation of relative surface area abundances of goethite and kaolinite, simulations were performed under the same chemical conditions as in Figure 3c, and the results are presented in Figure 3d. Figure 3d indicates that 100% goethite surface resulted in an overprediction of U(VI) adsorption in the pH range of 4.0−6.0, and 100% kaolinite surface resulted in an overprediction of adsorption at pH < 4.0. When the goethite

surface contribution was varied between 10%-30%, with the remaining surface area attributed to kaolinite, similar predictions were obtained that fit the experimental data nearly equally well. This is consistent with the fact that similar U(VI) adsorption edges were obtained for the fine fractions of sediments-A and -B (Figures 2c,d, 3c,d), even though they contain different abundances of goethite (17%, 27%) and kaolinite (83%, 73%) (Table 1). The model sensitivity analysis indicates that both goethite and kaolinite surfaces contributed to U(VI) adsorption under acidic pH conditions.

U(VI)/Bulk Sediments. The bulk sediment-A sample adsorbed U(VI) more (Figure 4a) than bulk sediment-B (Figure 4b) at pH $\leq$ 5.0. This is consistent with our conclusion that the fine fractions adsorb almost all of the U(VI), because the fine fraction content of sediment-A (13.0%) is greater than that of sediment-B (5.5%) (Table 1). The model simulations in Figure 4 for the bulk sediments were completed using the same SCM-CA model (Table 2). The total reactive surface areas in the bulk sediments were assumed to be contributed by the fine fractions because the SSA analysis (Table 1) indicates that ~100% of the surface area was associated with the fine fractions. Figure 4 shows that U(VI) adsorption behavior onto the bulk sediments can be predicted reasonably well using the SCM-CA model developed in this work.

As illustrated in Figure 4 as well as in Figure 3c, the predicted distribution of each surface species indicates that both goethite and kaolinite surfaces cocontributed to U(VI) adsorption under F-Area relevant pH conditions ($\leq$5.5). Specifically, the exchange sites from kaolinite play an dominant role in adsorption of U(VI) (i.e., $>X_2UO_2$) at pH $\leq$ 4.0, the edge site from goethite and kaolinite plus the exchange sites cocontribute for U(VI) adsorption (i.e., $(>FeOH)_2UO_2^+$, $(>FeOH)_2UO_2CO_3^-$, $(>SOH)_2UO_2^+$, $(>SOH)_2UO_2CO_3^-$ and $>X_2UO_2$) at pH 4.0–6.0, and goethite dominates U(VI) adsorption (i.e., $(>FeOH)_2UO_2CO_3^-$) at neutral and weakly alkaline pH conditions (6.0–8.5).

Application of the SCM-CA Model. This study reveals that SCMs developed from reference minerals are able to predict U(VI) adsorption behavior for relatively simple aquifer sediments such as the SRS F-Area background sediments. Our simple CA modeling approach provided useful information on the contributions of individual minerals and specific surface species for U(VI) adsorption under varying chemical conditions. The advantages of the CA modeling approach are that the SCMs and model parameters from reference mineral components are transferable from one field site to another and that the required models and parameters can be developed from detailed experimental investigations or obtained from publications in the literature.[4] However, application of the CA modeling approach to sediments and soils with mixed mineral assemblages has been limited due to the difficulty in estimating the relative accessible surface area abundances of reference mineral phases in sediments. As shown in this work, development of an experimental methodology for determining the relative surface area abundances of the reactive minerals in aquifer sediments is a significant new advance that may allow successful applications of this modeling approach at other field sites. Our humic acid method would be expected to work well in other low organic, quartz-dominated systems.

■ ASSOCIATED CONTENT

Ⓢ Supporting Information

The aqueous reactions and constants, the aqueous U(VI) speciation modeling, the concentrations of Al, Ca, Mg, Na, K, and Si in adsorption solutions, the detailed method for determining the relative surface area abundances of goethite and kaolinite in the fine fraction of sediment-A, and a comparison of selected experimental and modeling data are also available. This material is available free of charge via the Internet at http://pubs.acs.org.

■ AUTHOR INFORMATION

Corresponding Author

*Phone: 510-486-6004; fax: 510-486-7152; e-mail: jwan@lbl.gov.

■ ACKNOWLEDGMENTS

The work reported here is supported as part of the Sustainable Systems (SS) Scientific Focus Area (SFA) program at LBNL, supported by the U.S. Department of Energy, Office of Science, Office of Biological and Environmental Research, Subsurface Biogeochemical Research Program, through Contract No. DE-AC02-05CH11231 between Lawrence Berkeley National Laboratory and the U.S. Department of Energy. We thank Dr. Miles Denham for providing us the sediment samples from the Savannah River Site, and the anonymous reviewers for their helpful comments.

■ REFERENCES

(1) Wan, J.; Dong, W.; Tokunaga, T. K. Method to attenuate U(VI) mobility in acidic waste plumes using humic acids. *Environ. Sci. Technol.* **2011**, *45* (6), 2331–2337.

(2) Serkiz, S. M.; Johnson, W. H.; Wile, L. M. J.; Clark, S. B. Environmental availability of uranium in an acidic plume at the Savannah River Site. *Vadose Zone J.* **2007**, *6* (2), 354–362.

(3) Wan, J.; Tokunaga, T. K.; Dong, W.; Denham, M. E.; Hubbard, S. S., Understanding and predicting groundwater contaminant plumes: The F-Area, Savannah River Site. *Environ. Sci. Technol.* **Submitted**.

(4) Davis, J. A.; Meece, D. E.; Kohler, M.; Curtis, G. P. Approaches to surface complexation modeling of uranium(VI) adsorption on aquifer sediments. *Geochim. Cosmochim. Acta* **2004**, *68* (18), 3621–3641.

(5) McKinley, J. P.; Zachara, J. M.; Smith, S. C.; Turner, G. D. The influence of uranyl hydrolysis and multiple site-binding reactions on adsorption of U(VI) to montmorillonite. *Clays Clay Miner.* **1995**, *43* (5), 586–598.

(6) Waite, T. D.; Davis, J. A.; Payne, T. E.; Waychunas, G. A.; Xu, N. Uranium(VI) adsorption to ferrihydrite: Application of a surface complexation model. *Geochim. Cosmochim. Acta* **1994**, *58*, 5465–5478.

(7) Turner, G. D.; Zachara, J. M.; McKinley, J. P.; Smith, S. C. Surface-charge properties and UO_2^{2+} adsorption of a subsurface smectite. *Geochim. Cosmochim. Acta* **1996**, *60* (18), 3399–3414.

(8) Hsi, C. K. D.; Langmuir, D. Adsorption of uranyl onto ferric oxyhydroxides: Application of the surface complexation site-binding model. *Geochim. Cosmochim. Acta* **1985**, *49* (9), 1931–1941.

(9) Parkhurst, D. L.; Appelo, C. A. J. *User's Guide to PHREEQC (Version 2)—A Computer Program for Speciation, Batch-Reaction, One-Dimensional Transport, and Inverse Geochemical Calculations*; U.S. Geological Survey: Denver, CO, 2004.

(10) Dong, W.; Ball, W. P.; Liu, C.; Wang, Z.; Stone, A. T.; Bai, J.; Zachara, J. M. Influence of calcite and dissolved calcium on uranium(VI) sorption to a Hanford subsurface sediment. *Environ. Sci. Technol.* **2005**, *39* (20), 7949–7955.

(11) Shang, J.; Liu, C.; Wang, Z.; Zachara, J. M. Effect of grain size uranium(VI) surface complexation kinetics and adsorption additivity. *Environ. Sci. Technol.* **2011**, *45* (14), 6025–6031.

(12) Tao, Z.; Dong, W. Additivity rule and its application to the sorption of radionuclides on soils. *Radiochim. Acta* **2003**, *91* (5), 299–303.
(13) Langmuir, D., *Aqueous Environmental Geochemistry*; Prentice Hall: New Jersey, 1997.
(14) Heidmann, I.; Christl, I.; Leu, C.; Kretzschmar, R. Competitive sorption of protons and metal cations onto kaolinite: experiments and modeling. *J. Colloid Interface Sci.* **2005**, *282* (2), 270–282.
(15) Sherman, D. M.; Peacock, C. L.; Hubbard, C. G. Surface complexation of U(VI) on goethite (alpha-FeOOH). *Geochim. Cosmochim. Acta* **2008**, *72* (2), 298–310.
(16) Lund, T. J.; Koretsky, C. M.; Landry, C. J.; Schaller, M. S.; Das, S. Surface complexation modeling of Cu(II) adsorption on mixtures of hydrous ferric oxide and kaolinite. *Geochem. Trans.* **2008**, *9*.
(17) Reich, T. J.; Koretsky, C. M.; Das, S.; Lund, T. J.; Landry, C. J. Surface complexation modeling of Pb(II) adsorption on mixtures of hydrous ferric oxide, quartz and kaolinite. *Chem. Geol.* **2010**, *275* (3–4), 262–271.
(18) Villalobos, M.; Trotz, M. A.; Leckie, J. O. Surface complexation modeling of carbonate effects on the adsorption of Cr(VI), Pb(II), and U(VI) on goethite. *Environ. Sci. Technol.* **2001**, *35* (19), 3849–3856.
(19) Barnett, M. O.; Jardine, P. M.; Brooks, S. C. U(VI) adsorption to heterogeneous subsurface media: Application of a surface complexation model. *Environ. Sci. Technol.* **2002**, *36* (5), 937–942.
(20) Dzombak, D. A.; Morel, F. M. M., *Surface Complexation Modeling: Hydrous Ferric Oxide*; John Wiley & Sons: New York, 1990.
(21) Dong, W.; Brooks, S. C. Determination of the formation constants of ternary complexes of uranyl and carbonate with alkaline earth metals (Mg^{2+}, Ca^{2+}, Sr^{2+}, and Ba^{2+}) using anion exchange method. *Environ. Sci. Technol.* **2006**, *40* (15), 4689–4695.
(22) Dong, W.; Brooks, S. C. Formation of aqueous $MgUO_2(CO_3)_3^{2-}$ complex and uranium anion exchange mechanism onto an exchange resin. *Environ. Sci. Technol.* **2008**, *42* (6), 1979–1983.
(23) Fox, P. M.; Davis, J. A.; Zachara, J. M. The effect of calcium on aqueous uranium(VI) speciation and adsorption to ferrihydrite and quartz. *Geochim. Cosmochim. Acta* **2006**, *70* (6), 1379–1387.
(24) Moll, H.; Geipel, G.; Brendler, V.; Bernhard, G.; Nitsche, H. Interaction of uranium(VI) with silicic acid in aqueous solutions studied by time-resolved laser-induced fluorescence spectroscopy (TRLFS). *J. Alloys Compd.* **1998**, *271*, 765–768.
(25) Mahoney, J. J.; Cadle, S. A.; Jakubowski, R. T. Uranyl adsorption onto hydrous ferric oxide-A re-evaluation for the diffuse layer model database. *Environ. Sci. Technol.* **2009**, *43* (24), 9260–9266.
(26) Tao, Z.; Dong, W. Comparison between the one pK and two pK models of the metal oxide water interface. *J. Colloid Interface Sci.* **1998**, *208* (1), 248–251.
(27) Kulik, D. A., Standard molar Gibbs energies and activity coefficients of surface complexes on mineral-water interfaces (thermodynamic insights). In *Surface Complexation Modeling. Interface Sciences and Technology*; Lutzenkirchen, J., Ed.; Elsevier: Amsterdam, 2006; Vol. *11*, pp 171–250.
(28) Sverjensky, D. A. Standard states for the activities of mineral surface sites and species. *Geochim. Cosmochim. Acta* **2003**, *67* (1), 17–28.
(29) Kowal-Fouchard, A.; Drot, R.; Simoni, E.; Ehrhardt, J. J. Use of spectroscopic techniques for uranium(VI)/montmorillonite interaction modeling. *Environ. Sci. Technol.* **2004**, *38* (5), 1399–1407.
(30) Pabalan, R. T.; Turner, D. R. Uranium(6+) sorption onto montmorillonite: Experimental and surface complexation modeling. *Aquatic Geochem.* **1997**, *2*, 203–226.
(31) Zachara, J. M.; Mckinley, J. P. Influence of hydrolysis on the sorption of metal-cations by smectites—Importance of edge coordination reactions. *Aquatic Sci.* **1993**, *55* (4), 250–261.
(32) Sylwester, E. R.; Hudson, E. A.; Allen, P. G. The structure of uranium(VI) sorption complexes on silica, alumina, and montmorillonite. *Geochim. Cosmochim. Acta* **2000**, *64* (14), 2431–2438.
(33) Catalano, J. G.; Brown, Jr., G. E. Uranyl adsorption onto montmorillonite: Evaluation of binding sites and carbonate complexation. *Geochim. Cosmochim. Acta* **2005**, *69* (12), 2995–3005.
(34) Arai, Y.; McBeath, M.; Bargar, J. R.; Joye, J.; Davis, J. A. Uranyl adsorption and surface speciation at the imogolite-water interface: Self-consistent spectroscopic and surface complexation models. *Geochim. Cosmochim. Acta* **2006**, *70* (10), 2492–2509.
(35) Heidmann, I.; Christl, I.; Kretzschmar, R. Sorption of Cu and Pb to kaolinite-fulvic acid colloids: Assessment of sorbent interactions. *Geochim. Cosmochim. Acta* **2005**, *69* (7), 1675–1686.
(36) Pabalan, R. T.; Turner, D. R.; Bertetti, F. P.; Prikryl, J. D., Uranium(VI) Sorption onto Selected Mineral Surfaces: Key geochemical factors. In *Adsorption of Metals by Geomedia: Variables, Mechanisms and Model Applications*; Jenne, E. A., Ed.; Academic Press: San Diego, 1998; pp 99–130.
(37) Payne, T. E.; Davis, J. A.; Lumpkin, G. R.; Chisari, R.; Waite, T. D. Surface complexation model of uranyl sorption on Georgia kaolinite. *Appl. Clay Sci.* **2004**, *26* (1–4), 151–162.
(38) Davis, J. A.; Coston, J. A.; Kent, D. B.; Fuller, C. C. Application of the surface complexation concept to complex mineral assemblages. *Environ. Sci. Technol.* **1998**, *32* (19), 2820–2828.
(39) Kohler, M.; Curtis, G. P.; Meece, D. E.; Davis, J. A. Methods for estimating adsorbed uranium(VI) and distribution coefficients of contaminated sediments. *Environ. Sci. Technol.* **2004**, *38* (1), 240–247.

DISCLAIMER

DE-AC02-05CH11231